THE JOURNAL OF PHYSICAL CHEMISTRY B

Article

pubs.acs.org/JPCB

Insights into the Structural Changes Occurring upon Photoconversion in the Orange Carotenoid Protein from Broadband Two-Dimensional Electronic Spectroscopy

Eleonora De Re,[†,‡] Gabriela S. Schlau-Cohen,[‡,§,⊥] Ryan L. Leverenz,[§,∥] Vanessa M. Huxter,[‡,§,¶] Thomas A. A. Oliver,[‡,§] Richard A. Mathies,[§] and Graham R. Fleming*[,†,‡,§]

[†]Applied Science and Technology Graduate Group, University of California, Berkeley, California 94720, United States

[‡]Physical Biosciences Division, Lawrence Berkeley National Laboratory, Berkeley, California 94720, United States

[§]Department of Chemistry, University of California, Berkeley, California 94720, United States

Supporting Information

ABSTRACT: Carotenoids play an essential role in photoprotection, interacting with other pigments to safely dissipate excess absorbed energy as heat. In cyanobacteria, the short time scale photoprotective mechanisms involve the photoactive orange carotenoid protein (OCP), which binds a single carbonyl carotenoid. Blue-green light induces the photoswitching of OCP from its ground state form (OCPO) to a metastable photoproduct (OCPR). OCPR can bind to the phycobilisome antenna and induce fluorescence quenching. The photoswitching is accompanied by structural and functional changes at the level of the protein and of the bound carotenoid. Here, we use broadband two-dimensional electronic spectroscopy to study the differences in excited state dynamics of the carotenoid in the two forms of OCP. Our results provide insight into the origin of the pronounced vibrational lineshape and oscillatory dynamics observed in linear absorption and 2D electronic spectroscopy of OCPO and the large inhomogeneous broadening in OCPR, with consequences for the chemical function of the two forms.

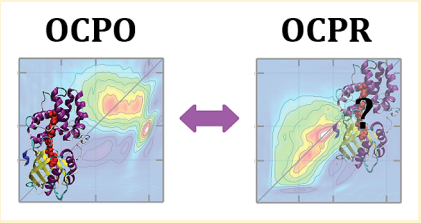

INTRODUCTION

Light absorption can be dangerous to photosynthetic organisms when it exceeds their capability to convert light energy into chemical energy. To avoid formation of damaging species upon excess light absorption, photosynthetic organisms adopt a series of mechanisms to dissipate light energy safely as heat, collectively referred to as non-photochemical quenching (NPQ). Carotenoids play a critical role in NPQ, as validated by a variety of biochemical,[1,2] spectroscopic,[3−7] and theoretical studies.[8,9] The mechanistic role of carotenoids in NPQ, however, is still not fully understood.[10] In cyanobacteria, excess light absorption induces a photoprotective mechanism that involves a carotenoid-binding photoactive protein, the orange carotenoid protein (OCP), which both senses light intensity and directly triggers photoprotection.[11−13]

OCP is a soluble 35 kDa protein found in the inter-thylakoid region, on the same side of the membrane as the phycobilisome antenna, the major light harvester in cyanobacteria.[12,14] OCP noncovalently binds a single pigment, the carotenoid 3′-hydroxyechinenone (3′-hECN). Absorption of blue-green light by OCP induces conformational changes in both the pigment and the protein, as experimentally demonstrated by Raman, FTIR experiments, and native mass spectrometry.[15,16] These changes convert the protein from its dark stable photoactive form, the orange OCPO, to a metastable form, the red OCPR. OCPR has been suggested to adopt an "open" conformation with increased accessibility of the carotenoid to solvent[17−20] and a weaker protein−carotenoid binding interaction.[16] OCPR has been shown to bind to the phycobilisome antenna and induce fluorescence quenching.[12,15,21] Isolated OCPR spontaneously converts back to the orange form in darkness, and the back-conversion kinetics are independent of illumination but very sensitive to temperature. The conversion takes a few seconds at room temperature (298 K) and ∼40 min at 283 K.[15]

OCPO binds the carotenoid 3′-hECN in an all-trans configuration (see Figure 1a).[14] The carbonyl on the 4-keto-β-ionylidene ring of 3′-hECN forms hydrogen bonds at the C-terminal domain of the protein. This carbonyl group is essential for OCP photoactivity, as OCP with zeaxanthin or β-carotene bound (which do not have a carbonyl group) is unable to photoconvert.[22] The roles of specific pigment−protein interactions responsible for tuning the spectroscopic and photochemical properties of 3′-hECN in OCP remain largely uncharacterized. Moreover, the conformation of the carotenoid and its interactions with the surrounding protein in OCPR are not conclusively known, as crystal and NMR structures are unavailable for this form.

In this paper, we investigate the photophysics of 3′-hECN in the two forms of OCP using two-dimensional electronic spectroscopy (2DES) to understand how the protein environ-

Received: February 28, 2014
Revised: April 25, 2014
Published: April 29, 2014

   dx.doi.org/10.1021/jp502120h | J. Phys. Chem. B 2014, 118, 5382−5389

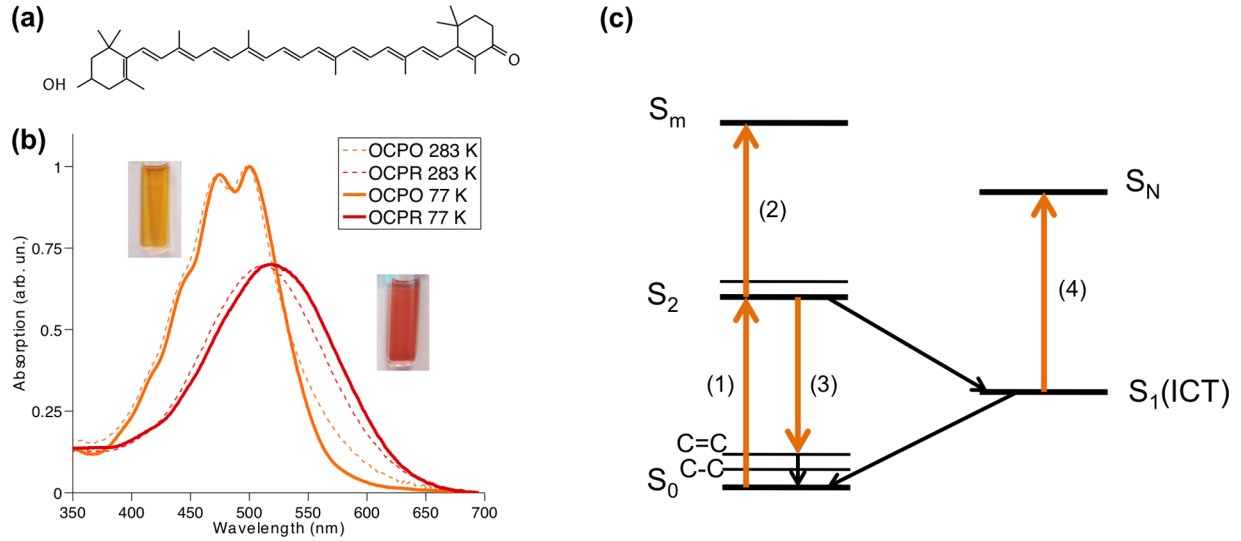

Figure 1. (a) Structure of the carotenoid 3′-hECN in the protein pocket in OCPO.[43] (b) Normalized linear absorption spectra of OCPO (orange line) and OCPR (red line) at 283 K (dashed line) and at 77 K (solid line). Pictures of the cuvettes containing the samples are shown next to the corresponding absorption spectra. (c) Energy level scheme of the key transitions within the main molecular pathways for the carotenoid 3′-hECN. The numbered transitions are: (1) $S_0 \rightarrow S_2$ ground-state bleach; (2) $S_2 \rightarrow S_m$ excited-state absorption; (3) S_2 emission; (4) S_1 excited-state absorption. The experimentally observable transitions are described for the two forms of OCP in the text.

ment modulates the pigment energetics and dynamics in OCPO and OCPR and relate this to the different biological function of the two forms (photoactive vs quenching). OCP is an ideal minimal system for the study of protein−pigment interactions, as it binds a single carotenoid. In contrast to other pigment−protein complexes that bind both carotenoids and chlorophyll pigments, the optical response of this minimal system is not complicated by inter-chromophore interactions, allowing direct observation of how the protein environment tunes and alters the properties of the pigment. Carotenoid photophysics are highly dependent both on the structure of the pigment and on the surrounding environment.[23] Therefore, observed differences in the photophysics of the two forms of OCP must arise from changes in the structure of the carotenoid bound to the protein pocket and in the pigment−protein binding interaction.

Previous time-resolved fluorescence[24] and transient absorption experiments[19,25,26] have investigated the mechanism played by OCP in energy dissipation. Transient absorption experiments in the visible region[19,25] suggested that OCPR could accept excitation energy from the phycobilisome bilin S_1 state to the carotenoid intramolecular charge transfer (ICT) state. The ICT state can subsequently relax to the ground state directly or via the S_1 state of 3′-hECN and then decay. Many open questions remain about the molecular origin of the different spectroscopic behavior observed for OCPO and OCPR. For example, the origin of the broadness and red shifting of the OCPR linear absorption has not been fully elucidated, and the origin of the ICT character enhancement in OCPR[19,25] is incompletely described.

2DES presents numerous advantages over other nonlinear spectroscopic techniques such as transient absorption (for recent reviews, see refs 27−30). 2DES affords time and spectral resolution over both excitation and emission processes and has been very successful in unraveling the complicated structure−function relationship of natural photosynthetic systems.[31−35] Broadband 2DES probing the visible region allows us to investigate and disentangle a spectral region usually congested in carotenoid photophysics and simultaneously provides the time resolution to investigate the ultrafast processes associated with the excited-state relaxation of carotenoids.[36]

Our 2DES results for the two forms of OCP are remarkably different. OCPO shows pronounced vibrational dynamics, while OCPR gives a highly inhomogeneously broadened signal. We discuss how the differences in protein environment for the carotenoid in the two forms might relate to their specific biological roles (photoactivity and quenching).

EXPERIMENTAL METHODS

Sample Preparation. OCP was purified from a frozen paste of *Arthrospira platensis* cells (a generous gift of Dr. Gerald Cysewski, Cyanotech Corporation) using a procedure similar to that described by Holt and Krogmann,[37] with isoelectric focusing omitted. Following anion exchange and gel filtration chromatography, the purified OCP had an A496/A280 ratio of 1.8:1. To prepare OCP for spectroscopic measurements, purified OCP in 50 mM Tris-HCl, 100 mM NaCl, pH 8 (24 °C) was concentrated to OD 30/cm in a centrifugal spin concentrator. For the OCPR sample, a 30 μL volume of concentrated OCP was initially converted to OCPR by 15 min of illumination with a 505 nm LED (Luxeon Rebel LXML-PE01-0070, Philips Lumileds, 40 nm FWHM) at 273 K. The illuminated sample was thoroughly mixed with 70 μL of chilled glycerol and illuminated for an additional 5 min. The sample was then transferred to a 200 μm path length quartz cuvette and cooled to 77 K in an optical cryostat (Oxford Instruments). The OCPR sample was continuously illuminated with the LED during the cooling to cryogenic temperature. The OCPO sample was prepared similarly but in complete darkness. The maximum OD was 0.28 at 502 nm for the OCPO sample and 0.25 at 518 nm for the OCPR sample. Linear absorption traces were collected before and after every 2DES measurement to check for sample stability at 77 K, and no measurable difference was observed in either sample. We cannot exclude a minor presence of RCP (red carotenoid protein[12,37,38]) in our OCP preparations based on the linear absorption alone. However, its

dx.doi.org/10.1021/jp502120h | J. Phys. Chem. B 2014, 118, 5382−5389

contribution would be the same in both OCPO and OCPR spectra, and we do not expect it to contribute to any observed differences in the dynamics of 3′-hECN in the two forms.

Two-Dimensional Electronic Spectroscopy. The 2DES experimental apparatus has been described in detail previously.[36,39,40] A home-built Ti:sapphire regenerative amplifier laser system pumped a home-built noncollinear optical parametric amplifier, producing laser pulses centered at 540 nm (550 nm for OCPR measurements) with 60 nm FWHM. The combination of a prism compression line followed by a diffraction-based SLM (spatial light modulator) pulse shaper compressed the pulses to a duration of 12 fs, as characterized by TG-FROG (transient grating frequency-resolved optical gating).[41] The beam was split into two replicas by a beam splitter, delayed with respect to each other via a retroreflector delay stage; this allowed the control of the waiting time T between pulses 2 and 3. The two beam pairs were further split into a total of four beams by a diffractive optic optimized for first-order diffraction, allowing for passive phase stabilization.[39] The delay between pulses 1 and 2, which corresponds to the coherence time τ, was implemented by means of movable glass wedges, allowing for interferometric precision in the control of τ.[39]

The beams were focused to the sample position in a box geometry and had an energy of ∼10 nJ per pulse. The interaction with pulses 1, 2, and 3 generates a third-order signal in the phase-matched direction, $\vec{k}_s = -\vec{k}_1 + \vec{k}_2 + \vec{k}_3$, collinear with beam 4, the local oscillator (attenuated by 4 orders of magnitude as to prevent any strong interaction with the sample). This signal was spectrally dispersed and heterodyne-detected on a CCD camera.

The coherence time τ was scanned from −360 to +360 fs in 0.8 fs time steps for fixed values of waiting time T. The resulting array of interferograms collected for each value of T was Fourier-transformed to produce the final 2DES spectrum. Negative values of the coherence time generated the non-rephasing signal (free induction decay), while positive coherence times generated the rephasing signal (photon echo signal). The two signals were obtained experimentally by inverting the ordering of pulses 1 and 2. The total 2DES spectrum, the relaxation spectrum, corresponds to the combined rephasing and non-rephasing components.

Dynamics were monitored by varying the waiting time T; spectra were collected every 10 fs from 0 to 100 fs, then at 120, 150, 300, 450, 1000, 2000, 5000, 7000, 10000, 15000, and 20000 fs. In order to phase the 2DES data, spectrally resolved pump−probe experiments were collected separately for the same values of T under the same experimental conditions.[40,42]

RESULTS

Linear Absorption. Figure 1b shows the linear absorption spectrum of the two forms of OCP at 283 and 77 K. OCPO, represented by an orange line, has resolvable features that correspond to the vibronic structure of the optically bright S_0−S_2 transition. The 0−0 transition is at 499 nm at 283 K and is red-shifted to 502 nm at 77 K. The OCPO sample appears orange, as shown in the inset on the left in Figure 1b. The structure of 3′-hECN in OCP is shown in Figure 1a.[43] The linear absorption spectrum at 283 K is asymmetrically broadened toward longer wavelengths. This broadening is reduced in the 77 K spectrum.

Upon blue-green light illumination, the absorption spectrum broadens and red-shifts. The main peak for the red form OCPR is at 512 nm at 283 K and red shifts to 522 nm at 77 K. The vibrational structure that was visible in OCPO is lost, and the spectrum appears nearly Gaussian, as seen in Figure 1b. No apparent band narrowing or increased resolution of vibronic structure is observed in the OCPR spectrum at 77 K.

Two-Dimensional Electronic Spectroscopy of OCPO. Figure 2a shows the laser spectrum used in the experiment, superimposed on the absorption spectrum of OCPO at 77 K. The laser pulse is resonant with the S_0−S_2 electronic transition of the carotenoid, covering the 0−0 vibrational transition and the red edge of the 0−1 transition.

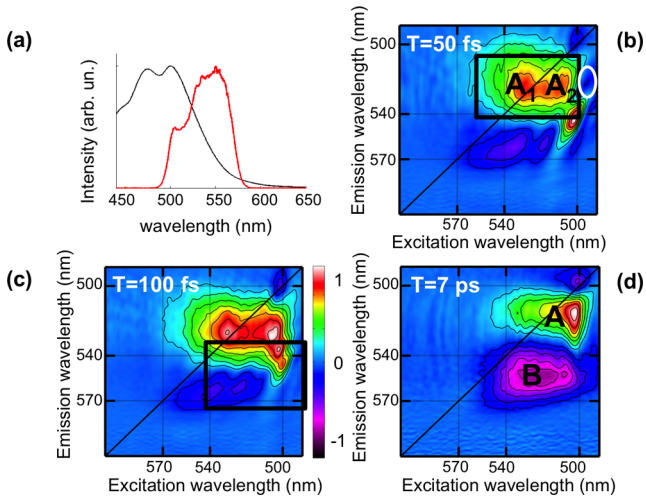

Figure 2. (a) Linear absorption spectrum of OCPO at 77 K (black line) and laser spectrum used in the experiment (red line). (b−d) Real-valued relaxation 2DES spectra of OCPO for selected waiting times T. Each 2DES spectrum throughout the paper is normalized to its own maximum. Positive signals are displayed in red and green, negative signals in purple and blue (see color bar). The letters and boxes highlight key peaks described in the text.

Figure 2b−d displays representative 2DES real-valued relaxation spectra of OCPO. The corresponding absolute-valued spectra are shown in the Supporting Information. Spectra acquired at long waiting times T (see T = 7 ps in Figure 2d) have two main features, A and B, with opposite signs. Short time spectra (T < 1 ps) are more complex (see Figure 2b,c), with multiple overlapping positive and negative features.

The laser pulse excites the system into the S_2 state; the positive feature centered around 515 nm (boxed region in Figure 2b) is assigned to a ground-state bleach (GSB)/stimulated emission (SE) signal from the $S_2 \rightarrow S_0$ transition (see Figure 1c for the energy level scheme). At early waiting times T, we observe the presence of a negative signal centered around 502 nm excitation and 527 nm emission (see Figure 2b, circled region in T = 50 fs spectrum). At this waiting time, the negative signal has mostly decayed, so it appears blue-shifted along the excitation axis, as the bleach signal becomes stronger. Given the spectral position of this negative band and the time scale of decay (the signal disappears after ∼50 fs), we assign it to an $S_2 \rightarrow S_m$ excited-state absorption (ESA). ESA from S_2 has previously been observed in the visible region in 2DES experiments on β-carotene in solution.[36,44] As the decay of the S_2 ESA signal proceeds, we see the appearance of two separate regions of intensity in the GSB/SE band, labeled A_1 and A_2 in the T = 50 fs spectrum in Figure 2b. A_1 and A_2 have an energy separation of ∼1000 cm^{-1}, and they oscillate in

dx.doi.org/10.1021/jp502120h | J. Phys. Chem. B 2014, 118, 5382−5389

intensity with a period of ~30 fs. The integrated intensity of the 2DES relaxation spectra in regions A_1 and A_2 is plotted as a function of waiting time T in Figure 3. The oscillation

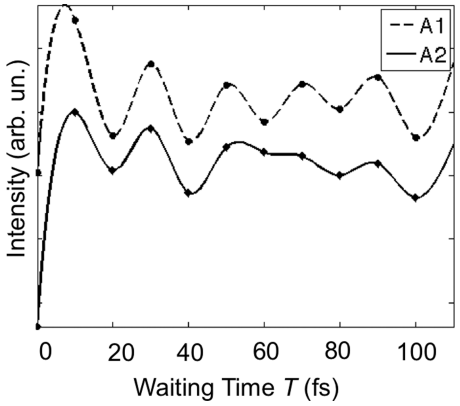

Figure 3. Evolution in time of the integrated intensity from the 2D spectra for regions centered at λ_t = 527 nm, labeled as A_1 and A_2 in Figure 2b.

frequency is close to the frequencies of C=C and C−C stretching of the ground state of the carotenoid 3′-hECN (21 and 28 fs, respectively[15]). We might also expect the intense 1008 cm^{-1} methyl rocking and 980 cm^{-1} hydrogen-out-of-plane (HOOP) wagging modes observed in prior Raman studies[15] to contribute to this oscillatory signal, the latter being unique to 3′-hECN in OCPO. The two peaks A_1 and A_2 are part of the same band and decay with the S_2 lifetime; therefore, they are most likely due to stimulated emission rather than ground-state bleach processes. They likely oscillate in phase due to the creation of ground-state wavepackets.

Even at early waiting times T, the A band (see Figure 2) is well rounded, meaning it does not exhibit any diagonal elongation. This can be explained as a very fast randomization on the S_2 potential energy surface of molecules that unsuccessfully pass through the conical intersection[45−47] with the S_1 state and are scattered in a range of trajectories.

At later times, the system undergoes ultrafast internal conversion to the S_1 state. A negative feature centered at λ_t = 550 nm (feature B, T = 7 ps spectrum in Figure 2d) appears, corresponding to $S_1 \rightarrow S_N$ ESA. The spectra at waiting times T larger than ~2 ps show little evolution of the two main GSB/SE and ESA features. By 20 ps, the signals have entirely decayed, corresponding to the complete relaxation of the population from S_1 to the ground state (spectra not shown).

At early times T, in the region of emission wavelengths between the GSB/SE and the ESA signals (emission wavelength between 535 and 565 nm), we observe the presence of additional positive and negative features, overlapping spectrally and evolving in time. This region is highlighted by a rectangular box in the T = 100 fs spectrum in Figure 2c. This spectral region would be difficult to resolve or interpret in a 1D transient absorption experiment (which integrates over the excitation axis), as there are multiple overlapping signals of opposite sign arising from S_2, S_1, and possible contributions from other states such as S*.[23,48−50] 2DES, however, can resolve the evolution of all these features and track them as a function of waiting time, T.

To understand the origin of these peaks, we refer to the rephasing and non-rephasing components of the early time spectra. Figure 4 shows the rephasing and non-rephasing components of the T = 100 fs spectrum, with a rectangular box highlighting the spectral region of interest. The rephasing spectrum shows a similar pattern to the relaxation spectrum in the boxed region, with alternating positive and negative peaks, while in the non-rephasing component, a single positive peak appears. The peaks are observable in the spectra for waiting times shorter than T = 1 ps (data not shown), longer than the S_2 lifetime.[19] A dispersive lineshape for cross-peaks in the rephasing component of 2DES spectra has been previously observed in both theoretical and experimental work.[36,44,51] This particular lineshape has been attributed to coupling of an electronic transition to a high frequency vibration. In 2DES experiments on β-carotene in solution, an analogous signal has been assigned to the population of a hot ground state via Impulsive Stimulated Raman Scattering (ISRS).[36] Given the similarity in dynamics, lineshape and spectral position of the cross-peaks in our spectra, we propose that they arise from the formation of a wavepacket on the hot ground state.

Two-Dimensional Electronic Spectroscopy of OCPR. Figure 5 shows absolute-valued 2DES spectra for selected waiting times T for OCPR at 77 K. Figure 6 shows real-valued spectra for T = 30 fs and 7 ps.[52] The laser pulse excites the $S_0 \rightarrow S_2$ transition, and a positive signal appears in the 2D spectra, corresponding to GSB/SE. After excitation, the S_2 population undergoes ultrafast internal conversion to the S_1 state, but the S_2 lifetime cannot be determined with precision. Due to the spectral position of our laser pulse, we are not able to observe the negative peak corresponding to the $S_1 \rightarrow S_N$ excited-state absorption signal in our 2D spectra. This ESA signal is in fact red-shifted in OCPR and falls outside the bandwidth of our laser pulse.[19,25] No additional features appear: the GSB/SE signal decays as the molecule relaxes back to S_0, and this relaxation is complete by 20 ps. The OCPR 2D spectra are

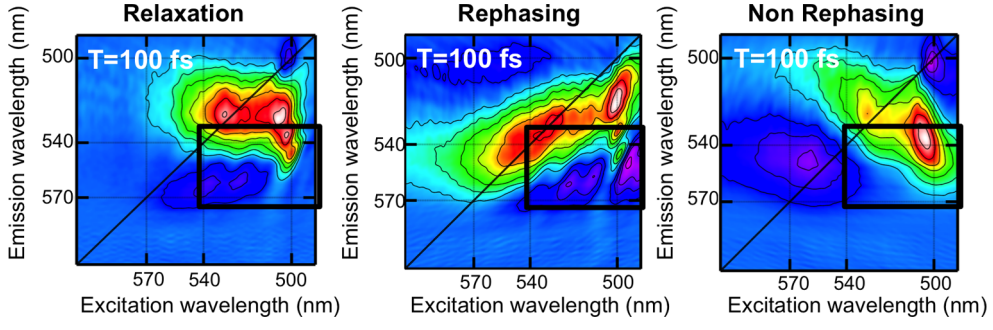

Figure 4. 2DES spectra of OCPO for T = 100 fs: relaxation, rephasing, and non-rephasing components.

dx.doi.org/10.1021/jp502120h | J. Phys. Chem. B 2014, 118, 5382−5389

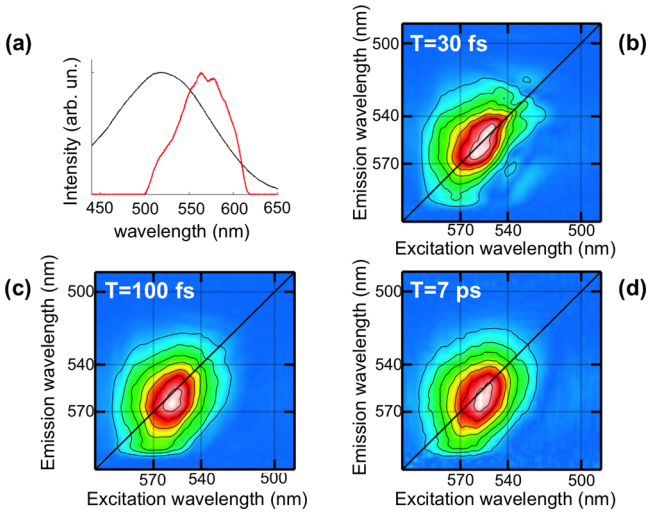

Figure 5. (a) Linear absorption spectrum of OCPR at 77 K (black line) and laser spectrum used in the experiment (red line). (b–d) Absolute-valued relaxation 2DES spectra of OCPR for selected waiting times T.

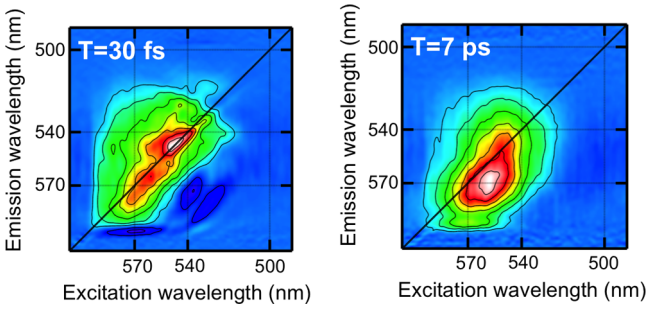

Figure 6. Real-valued 2DES spectra of OCPR for T = 30 fs and 7 ps.

significantly different from the OCPO 2D spectra, being structureless, as well as exhibiting no evidence of vibrational wavepackets on S_2 nor signatures of ISRS between S_0 and S_2.

The shape of the 2D spectra for the red form can help elucidate the origin of the broad static lineshape observed in the absorption spectrum (see Figure 1b). The OCPR spectra have a pronounced diagonal elongation (see the T = 30 fs spectrum in Figure 6), suggesting the large contribution of inhomogeneous broadening.

DISCUSSION

Linear Absorption. The origin of the asymmetric broadening toward lower energies in the 283 K OCPO spectrum has been previously assigned to the stabilization of the ICT state common to carbonyl carotenoids.[43] Conversely, a more recent study by Polivka et al.[26] assigns this to ground-state heterogeneity, assuming at room temperature the existence of a mixture of the two forms (OCPO, OCPR). Due to the observed reduction in asymmetric broadening at low energies in the 77 K versus the 283 K OCPO linear absorption, we believe that the low-energy broadening in the 283 K spectrum could be caused by either the thermal population of low-frequency vibrational modes with energies lower than k_BT (~200 cm^{-1} at 283 K) or a distribution of conformers resulting from rotations about C–C bonds in 3′-hECN.

Concurrently, no narrowing is observed in the OCPR spectra upon lowering of the temperature. The static lineshape is highly broadened in this form even at 77 K. Interestingly, previous studies have shown that even upon absence of the C-terminal domain the shape and width of the spectrum are unchanged.[20,53] This suggests that the origin of this particular lineshape is not highly dependent on the interactions between the C-terminal domain and the carbonyl group of 3′-hECN. Further investigation of the molecular origin of the static broadening will be provided in the discussion of the 2D results.

Two-Dimensional Electronic Spectroscopy. 2DES allows us to compare 3′-hECN photophysics in OCPO versus OCPR, decongesting vibrational and electronic dynamics occurring on femtosecond to picosecond time scales over ~100 nm bandwidth. Our ultrashort (<15 fs) pulses have allowed us to directly investigate with high time resolution the early time dynamics of 3′-hECN in the protein environment of OCP.

Vibrational activity is visible in both real and absolute-valued 2DES spectra of OCPO. Multiple vibrational modes are initially photoexcited on the S_2 state, and the action of ground-state wavepackets persists for up to ~1 ps. The 2DES results for OCPO resemble those obtained at cryogenic temperatures on β-carotene in a 2-methyl tetrahydrofuran glass.[36] OCPR, on the other hand, has no observable vibrational features and appears largely broadened, as expected from the linear absorption spectrum.

The precise molecular origin of the observed large inhomogeneous broadening requires further investigation. Conformational heterogeneity could play an important role if 3′-hECN is exposed to bulk solvent due to a loss of pigment–protein interactions attributed to the C-terminal domain of OCPO.[20] Solvent-induced broadening of the electronic absorption spectra of carbonyl carotenoids has previously been attributed to mixtures of conformational isomers preferentially formed in polar versus nonpolar solvents.[54,55] Exposure of the carbonyl group of 3′-hECN to bulk solvent may create a distribution of conformers at the carbonyl-containing end ring (from s-*trans*, as in OCPO, to s-*cis*, as in solution[26]). Additionally, fluctuations in the electrostatic environment of the chromophore produced by an ensemble of protein conformations or differences in H-bonding interactions with amino acids or water molecules could create a distribution of 0–0 energies that could further broaden the absorption spectrum of this form. Further experiments on OCP reconstituted with non-carbonyl carotenoids (such as β-carotene or zeaxanthin) and lacking the C-terminal domain could help disentangle these different possible contributions to the inhomogeneous broadening.

Our 2DES data on isolated OCP do not provide evidence for a direct role of 3′-hECN in OCPR-based quenching. We do not, for example, observe any significant shortening of the S_1 lifetime in OCPR versus OCPO, consistent with the results in ref 19, and while it is generally accepted that 3′-hECN plays a direct role in the quenching process,[24,56] the precise mechanism by which excess energy is dissipated remains under debate. 3′-hECN could play a direct role via energy or charge transfer,[19,24] or the OCPR complex could act allosterically to initiate quenching within the phycobilisome in analogy to the mechanism proposed for zeaxanthin in plant non-photochemical quenching by Horton et al.[57] Polivka et al.[26] recently determined only a small energetic advantage for the S_1 state of 3′-hECN in OCPR versus OCPO relative to the phycobilisome bilin S_1 state. We are not able to observe signatures of the ICT state in our data, due to the bandwidth of the laser pulse used,

dx.doi.org/10.1021/jp502120h | J. Phys. Chem. B 2014, 118, 5382–5389

and thus we cannot make conclusions on the enhancement of the ICT character for 3′-hECN in OCPR nor draw conclusions regarding its potential involvement in a quenching mechanism. Our data do, however, provide insight into the perturbed local environment provided by the protein pocket in OCPO and OCPR.

Interestingly, it has not been conclusively demonstrated that the 4-keto-β-ionylidene ring, nor the ICT state resulting from the presence of the conjugated carbonyl group, is necessary for quenching activity in an OCP−phycobilisome complex. Could the presence of the 4-keto group be more strictly required for photoactivity rather than quenching activity? OCP is a photoswitch, and the unique photochemistry of 3′-hECN in OCPO must be responsible for driving structural changes in the protein that ultimately lead to formation of the OCPR form, binding of OCP to the phycobilisome, and induction of the quenching mechanism. It is known that interactions between the 4-keto group and absolutely conserved residues in the C-terminal domain (Y203 and W290) are strictly required for OCP photoactivity.[22,58] While a relevant modulation of 3′-hECNs conformation(s) and/or photophysical properties in the OCPR form certainly may occur in the context of quenching activity, we must also consider the possibility that the photophysical properties of OCPR's 3′-hECN chromophore *in vitro* could simply arise as a secondary consequence of other mechanistically critical changes in protein structure and chromophore solvent accessibility that occur during the photochemical mechanism and allow OCP to bind to the phycobilisome. Further studies of the quenching complex formed by OCP bound to the phycobilisome antenna[21] are clearly needed to elucidate the specific nature of the quenching mechanism.

CONCLUSIONS

Here we have presented 2DES results comparing the excited-state dynamics of 3′-hECN in OCPO and OCPR. The study investigates the photophysics of a carbonyl carotenoid in two different electrostatic environments following photoconversion of the OCP holoprotein. Our results show resolvable and rich vibrational dynamics in OCPO, consistent with the carotenoid being held in a tightly locked conformation by the protein environment, with consequences for the photoactivity of this form. OCPR, on the other hand, shows a highly inhomogeneously broadened behavior. The origin of this large inhomogeneous broadening can be attributed to conformational heterogeneity due to exposure of the pigment to free solvent or to variations in the electrostatic environment experienced by the carotenoid. Further studies targeted to the investigation of the specific pigment−protein interactions in the C-terminal domain of OCP should help elucidate the role of the carbonyl group and the protein environment in tuning OCP photochemistry.

ASSOCIATED CONTENT

Supporting Information

Absolute-valued 2DES spectra for OCPO at selected waiting times. This material is available free of charge via the Internet at http://pubs.acs.org.

AUTHOR INFORMATION

Corresponding Author

*E-mail: grfleming@lbl.gov.

Present Addresses

[⊥](G.S.S.-C.) Department of Chemistry, Stanford University.
[∥](R.L.L.) Plant Research Lab, Michigan State University.
[¶](V.M.H.) Department of Chemistry and Biochemistry, University of Arizona.

Notes

The authors declare no competing financial interest.

ACKNOWLEDGMENTS

This work was supported by the Director, Office of Science, Office of Basic Energy Sciences, of the U.S. Department of Energy under Contract DE-AC02-05CH11231 and the Division of Chemical Sciences, Geosciences and Biosciences Division, Office of Basic Energy Sciences through Grant DE-AC03-76SF000098 (at LBNL and U.C. Berkeley). The authors acknowledge J. Zaks for helpful comments on the manuscript. The authors also thank Dr. Gerald Cysewski for the gift of *A. platensis* cells.

REFERENCES

(1) Niyogi, K. K.; Björkman, O.; Grossman, A. R. The Roles of Specific Xanthophylls in Photoprotection. *Proc. Natl. Acad. Sci. U.S.A.* **1997**, *94*, 14162−14167.
(2) Li, Z.; Ahn, T. K.; Avenson, T. J.; Ballottari, M.; Cruz, J. A.; Kramer, D. M.; Bassi, R.; Fleming, G. R.; Keasling, J. D.; Niyogi, K. K. Lutein Accumulation in the Absence of Zeaxanthin Restores Nonphotochemical Quenching in the *Arabidopsis thaliana* npq1 Mutant. *Plant Cell* **2009**, *21*, 1798−1812.
(3) Ruban, A. V.; Pascal, A. A.; Robert, B.; Horton, P. Activation of Zeaxanthin Is an Obligatory Event in the Regulation of Photosynthetic Light Harvesting. *J. Biol. Chem.* **2002**, *277*, 7785−7789.
(4) Ma, Y.-Z.; Holt, N. E.; Li, X.-P.; Niyogi, K. K.; Fleming, G. R. Evidence for Direct Carotenoid Involvement in the Regulation of Photosynthetic Light Harvesting. *Proc. Natl. Acad. Sci. U.S.A.* **2003**, *100*, 4377−4382.
(5) Holt, N. E.; Zigmantas, D.; Valkunas, L.; Li, X.-P.; Niyogi, K. K.; Fleming, G. R. Carotenoid Cation Formation and the Regulation of Photosynthetic Light Harvesting. *Science* **2005**, *307*, 433−436.
(6) Ruban, A. V.; Berera, R.; Ilioaia, C.; van Stokkum, I. H. M.; Kennis, J. T. M.; Pascal, A. A.; van Amerongen, H.; Robert, B.; Horton, P.; van Grondelle, R. Identification of a Mechanism of Photoprotective Energy Dissipation in Higher Plants. *Nature* **2007**, *450*, 575−578.
(7) Bode, S.; Quentmeier, C. C.; Liao, P.-N.; Hafi, N.; Barros, T.; Wilk, L.; Bittner, F.; Walla, P. J. On the Regulation of Photosynthesis by Excitonic Interactions between Carotenoids and Chlorophylls. *Proc. Natl. Acad. Sci. U.S.A.* **2009**, *106*, 12311−12316.
(8) Dreuw, A.; Fleming, G. R.; Head-Gordon, M. Chlorophyll Fluorescence Quenching by Xanthophylls. *Phys. Chem. Chem. Phys.* **2003**, *5*, 3247−3256.
(9) Dreuw, A.; Fleming, G. R.; Head-Gordon, M. Charge-Transfer State as a Possible Signature of a Zeaxanthin-Chlorophyll Dimer in the Non-photochemical Quenching Process in Green Plants. *J. Phys. Chem. B* **2003**, *107*, 6500−6503.
(10) Ruban, A. V.; Johnson, M. P.; Duffy, C. D. The Photoprotective Molecular Switch in the Photosystem II Antenna. *Biochim. Biophys. Acta* **2012**, *1817*, 167−181.
(11) Rakhimberdieva, M. G.; Stadnichuk, I. N.; Elanskaya, I. V.; Karapetyan, N. V. Carotenoid-Induced Quenching of the Phycobilisome Fluorescence in Photosystem II-Deficient Mutant of *Synechocystis* sp. *FEBS Lett.* **2004**, *574*, 85−88.
(12) Wilson, A.; Ajlani, G.; Verbavatz, J.-M.; Vass, I.; Kerfeld, C. A.; Kirilovsky, D. A Soluble Carotenoid Protein Involved in Phycobilisome-Related Energy Dissipation in Cyanobacteria. *Plant Cell* **2006**, *18*, 992−1007.
(13) Niyogi, K. K.; Truong, T. B. Evolution of Flexible Non-Photochemical Quenching Mechanisms that Regulate Light Harvest-

ing in Oxygenic Photosynthesis. *Curr. Opin. Plant Biol.* **2013**, *16*, 307−314.
(14) Kerfeld, C. A.; Sawaya, M. R.; Brahmandam, V.; Cascio, D.; Ho, K. K.; Trevithick-Sutton, C. C.; Krogmann, D. W.; Yeates, T. O. The Crystal Structure of a Cyanobacterial Water-Soluble Carotenoid Binding Protein. *Structure* **2003**, *11*, 55−65.
(15) Wilson, A.; Punginelli, C.; Gall, A.; Bonetti, C.; Alexandre, M.; Routaboul, J.-M.; Kerfeld, C. A.; van Grondelle, R.; Robert, B.; Kennis, J. T. M.; Kirilovsky, D. A Photoactive Carotenoid Protein Acting as Light Intensity Sensor. *Proc. Natl. Acad. Sci. U.S.A.* **2008**, *105*, 12075−12080.
(16) Zhang, H.; Liu, H.; Niedzwiedzki, D. M.; Prado, M.; Jiang, J.; Gross, M. L.; Blankenship, R. E. Molecular Mechanism of Photoactivation and Structural Location of the Cyanobacterial Orange Carotenoid Protein. *Biochemistry* **2014**, *53*, 13−19.
(17) Wilson, A.; Kinney, J. N.; Zwart, P. H.; Punginelli, C.; D'Haene, S.; Perreau, F.; Klein, M. G.; Kirilovsky, D.; Kerfeld, C. A. Structural Determinants Underlying Photoprotection in the Photoactive Orange Carotenoid Protein of Cyanobacteria. *J. Biol. Chem.* **2010**, *285*, 18364−18375.
(18) Wilson, A.; Gwizdala, M.; Mezzetti, A.; Alexandre, M.; Kerfeld, C. A.; Kirilovsky, D. The Essential Role of the N-Terminal Domain of the Orange Carotenoid Protein in Cyanobacterial Photoprotection: Importance of a Positive Charge for Phycobilisome Binding. *Plant Cell* **2012**, *24*, 1972−1983.
(19) Berera, R.; Gwizdala, M.; van Stokkum, I. H. M.; Kirilovsky, D.; van Grondelle, R. Excited States of the Inactive and Active Forms of the Orange Carotenoid Protein. *J. Phys. Chem. B* **2013**, *117*, 9121−9128.
(20) Leverenz, R. L.; Jallet, D.; Mathies, R. A.; Kirilovsky, D.; Kerfeld, C. A. Structural and Functional Modularity of the Orange Carotenoid Protein: Distinct Roles for the N-and C-Terminal Domains in Cyanobacterial Photoprotection. *Plant Cell* **2014**, *26*, 426−437.
(21) Gwizdala, M.; Wilson, A.; Kirilovsky, D. In Vitro Reconstitution of the Cyanobacterial Photoprotective Mechanism Mediated by the Orange Carotenoid Protein in *Synechocystis* PCC 6803. *Plant Cell* **2011**, *23*, 2631−2643.
(22) Punginelli, C.; Wilson, A.; Routaboul, J.-M.; Kirilovsky, D. Influence of Zeaxanthin and Echinenone Binding on the Activity of the Orange Carotenoid Protein. *Biochim. Biophys. Acta* **2009**, *1787*, 280−288.
(23) Polívka, T.; Sundström, V. Ultrafast Dynamics of Carotenoid Excited States—From Solution to Natural and Artificial Systems. *Chem. Rev.* **2004**, *104*, 2021−2071.
(24) Tian, L.; van Stokkum, I. H. M.; Koehorst, R. B. M.; Jongerius, A.; Kirilovsky, D.; van Amerongen, H. Site, Rate, and Mechanism of Photoprotective Quenching in Cyanobacteria. *J. Am. Chem. Soc.* **2011**, *133*, 18304−18311.
(25) Berera, R.; van Stokkum, I. H. M.; Gwizdala, M.; Wilson, A.; Kirilovsky, D.; van Grondelle, R. The Photophysics of the Orange Carotenoid Protein, a Light-Powered Molecular Switch. *J. Phys. Chem. B* **2012**, *116*, 2568−2574.
(26) Polívka, T.; Chábera, P.; Kerfeld, C. A. Carotenoid−Protein Interaction Alters the S_1 Energy of Hydroxyechinenone in the Orange Carotenoid Protein. *Biochim. Biophys. Acta* **2013**, *1827*, 248−254.
(27) Ginsberg, N. S.; Cheng, Y.-C.; Fleming, G. R. Two-Dimensional Electronic Spectroscopy of Molecular Aggregates. *Acc. Chem. Res.* **2009**, *42*, 1352−1363.
(28) Schlau-Cohen, G. S.; Ishizaki, A.; Fleming, G. R. Two-Dimensional Electronic Spectroscopy and Photosynthesis: Fundamentals and Applications to Photosynthetic Light-Harvesting. *Chem. Phys.* **2011**, *386*, 1−22.
(29) Lewis, K. L. M.; Ogilvie, J. P. Probing Photosynthetic Energy and Charge Transfer with Two-Dimensional Electronic Spectroscopy. *J. Phys. Chem. Lett.* **2012**, *3*, 503−510.
(30) Schlau-Cohen, G.; Dawlaty, J.; Fleming, G. Ultrafast Multidimensional Spectroscopy: Principles and Applications to Photosynthetic Systems. *IEEE J. Sel. Top. Quantum Electron.* **2012**, *18*, 283−295.
(31) Read, E. L.; Schlau-Cohen, G. S.; Engel, G. S.; Georgiou, T.; Papiz, M. Z.; Fleming, G. R. Pigment Organization and Energy Level Structure in Light-Harvesting Complex 4: Insights from Two-Dimensional Electronic Spectroscopy. *J. Phys. Chem. B* **2009**, *113*, 6495−6504.
(32) Schlau-Cohen, G. S.; Calhoun, T. R.; Ginsberg, N. S.; Read, E. L.; Ballottari, M.; Bassi, R.; van Grondelle, R.; Fleming, G. R. Pathways of Energy Flow in LHCII from Two-Dimensional Electronic Spectroscopy. *J. Phys. Chem. B* **2009**, *113*, 15352−15363.
(33) Schlau-Cohen, G. S.; Calhoun, T. R.; Ginsberg, N. S.; Ballottari, M.; Bassi, R.; Fleming, G. R. Spectroscopic Elucidation of Uncoupled Transition Energies in the Major Photosynthetic Light-Harvesting Complex, LHCII. *Proc. Natl. Acad. Sci. U.S.A.* **2010**, *107*, 13276−13281.
(34) Ginsberg, N. S.; Davis, J. A.; Ballottari, M.; Cheng, Y.-C.; Bassi, R.; Fleming, G. R. Solving Structure in the CP29 Light Harvesting Complex with Polarization-Phased 2D Electronic Spectroscopy. *Proc. Natl. Acad. Sci. U.S.A.* **2011**, *108*, 3848−3853.
(35) Schlau-Cohen, G. S.; De Re, E.; Cogdell, R. J.; Fleming, G. R. Determination of Excited-State Energies and Dynamics in the B Band of the Bacterial Reaction Center with 2D Electronic Spectroscopy. *J. Phys. Chem. Lett.* **2012**, *3*, 2487−2492.
(36) Calhoun, T. R.; Davis, J. A.; Graham, M. W.; Fleming, G. R. The Separation of Overlapping Transitions in β-Carotene with Broadband 2d Electronic Spectroscopy. *Chem. Phys. Lett.* **2012**, *523*, 1−5.
(37) Holt, T. K.; Krogmann, D. W. A Carotenoid−Protein from Cyanobacteria. *Biochim. Biophys. Acta* **1981**, *637*, 408−414.
(38) Wu, Y. P.; Krogmann, D. W. The Orange Carotenoid Protein of *Synechocystis* PCC 6803. *Biochim. Biophys. Acta* **1997**, *1322*, 1−7.
(39) Brixner, T.; Stiopkin, I. V.; Fleming, G. R. Tunable Two-Dimensional Femtosecond Spectroscopy. *Opt. Lett.* **2004**, *29*, 884−886.
(40) Brixner, T.; Mancal, T.; Stiopkin, I. V.; Fleming, G. R. Phase-Stabilized Two-Dimensional Electronic Spectroscopy. *J. Chem. Phys.* **2004**, *121*, 4221−4236.
(41) Trebino, R.; DeLong, K. W.; Fittinghoff, D. N.; Sweetser, J. N.; Krumbügel, M. A.; Richman, B. A.; Kane, D. J. Measuring Ultrashort Laser Pulses in The Time-Frequency Domain Using Frequency-Resolved Optical Gating. *Rev. Sci. Instrum.* **1997**, *68*, 3277−3295.
(42) Hybl, J. D.; Ferro, A. A.; Jonas, D. M. Two-Dimensional Fourier Transform Electronic Spectroscopy. *J. Chem. Phys.* **2001**, *115*, 6606−6622.
(43) Polívka, T.; Kerfeld, C. A.; Pascher, T.; Sundström, V. Spectroscopic Properties of the Carotenoid 3′-Hydroxyechinenone in the Orange Carotenoid Protein from the Cyanobacterium *Arthrospira maxima*. *Biochemistry* **2005**, *44*, 3994−4003.
(44) Christensson, N.; Milota, F.; Nemeth, A.; Sperling, J.; Kauffmann, H. F.; Pullerits, T.; Hauer, J. Two-Dimensional Electronic Spectroscopy of β-Carotene. *J. Phys. Chem. B* **2009**, *113*, 16409−16419.
(45) Garavelli, M.; Celani, P.; Bernardi, F.; Robb, M. A.; Olivucci, M. Force Fields for "Ultrafast" Photochemistry: The S_2 $(1B_u)$ → S_1 $(2A_g)$ → S_0 $(1A_g)$ Reaction Path for *all-trans*-Hexa-1,3,5-triene. *J. Am. Chem. Soc.* **1997**, *119*, 11487−11494.
(46) Fuss, W.; Haas, Y.; Zilberg, S. Twin States and Conical Intersections in Linear Polyenes. *Chem. Phys.* **2000**, *259*, 273−295.
(47) McCamant, D. W.; Kukura, P.; Mathies, R. A. Femtosecond Time-Resolved Stimulated Raman Spectroscopy: Application to the Ultrafast Internal Conversion in β-Carotene. *J. Phys. Chem. A* **2003**, *107*, 8208−8214.
(48) Gradinaru, C. C.; Kennis, J. T.; Papagiannakis, E.; van Stokkum, I. H.; Cogdell, R. J.; Fleming, G. R.; Niederman, R. A.; van Grondelle, R. An Unusual Pathway of Excitation Energy Deactivation in Carotenoids: Singlet-to-Triplet Conversion on an Ultrafast Timescale in a Photosynthetic Antenna. *Proc. Natl. Acad. Sci. U.S.A.* **2001**, *98*, 2364−2369.
(49) Wohlleben, W.; Buckup, T.; Hashimoto, H.; Cogdell, R. J.; Herek, J. L.; Motzkus, M. Pump-Deplete-Probe Spectroscopy and the

Puzzle of Carotenoid Dark States. *J. Phys. Chem. B* **2004**, *108*, 3320−3325.
(50) Polívka, T.; Sundström, V. Dark Excited States of Carotenoids: Consensus and Controversy. *Chem. Phys. Lett.* **2009**, *477*, 1−11.
(51) Mančal, T.; Nemeth, A.; Milota, F.; Lukeš, V.; Kauffmann, H. F.; Sperling, J. Vibrational Wave Packet Induced Oscillations in Two-Dimensional Electronic Spectra. II. Theory. *J. Chem. Phys.* **2010**, *132*, 184515.
(52) It was only possible to retrieve the phase factor from pump−probe data for 2DES spectra at select waiting times *T*, as shown in Figure 6. For comparison, absolute-valued OCPO spectra are shown in the Supporting Information.
(53) Chábera, P.; Durchan, M.; Shih, P. M.; Kerfeld, C. A.; Polívka, T. Excited-State Properties of the 16 kDa Red Carotenoid Protein from *Arthrospira maxima*. *Biochim. Biophys. Acta* **2011**, *1807*, 30−35.
(54) Shima, S.; Ilagan, R. P.; Gillespie, N.; Sommer, B. J.; Hiller, R. G.; Sharples, F. P.; Frank, H. A.; Birge, R. R. Two-Photon and Fluorescence Spectroscopy and the Effect of Environment on the Photochemical Properties of Peridinin in Solution and in the Peridinin-Chlorophyll-Protein from *Amphidinium carterae*. *J. Phys. Chem. A* **2003**, *107*, 8052−8066.
(55) Enriquez, M. M.; Fuciman, M.; LaFountain, A. M.; Wagner, N. L.; Birge, R. R.; Frank, H. A. The Intramolecular Charge Transfer State in Carbonyl-Containing Polyenes and Carotenoids. *J. Phys. Chem. B* **2010**, *114*, 12416−12426.
(56) Tian, L.; Gwizdala, M.; van Stokkum, I.; Koehorst, R.; Kirilovsky, D.; van Amerongen, H. Picosecond Kinetics of Light Harvesting and Photoprotective Quenching in Wild-Type and Mutant Phycobilisomes Isolated from the Cyanobacterium *Synechocystis* PCC 6803. *Biophys. J.* **2012**, *102*, 1692−1700.
(57) Horton, P.; Ruban, A. V.; Wentworth, M. Allosteric Regulation of the Light-Harvesting System of Photosystem II. *Philos. Trans. R. Soc., B* **2000**, *355*, 1361−1370.
(58) Wilson, A.; Punginelli, C.; Couturier, M.; Perreau, F.; Kirilovsky, D. Essential Role of Two Tyrosines and Two Tryptophans on the Photoprotection Activity of the Orange Carotenoid Protein. *Biochim. Biophys. Acta* **2011**, *1807*, 293−301.